

# Model Predictive Control-Based Active/Reactive Power Regulation of Inverter Air Conditioners for Improving Voltage Quality of Distribution Systems

Lunshu Chen<sup>ID</sup>, Student Member, IEEE, and Hongxun Hui<sup>ID</sup>, Member, IEEE

**Abstract**—The distribution system's voltage has more fluctuations due to the increasing intermittent and uncertain generation of renewable energy sources. To deal with massive and abrupt voltage issues, more operating reserves should be established. Compared with traditional regulation resources from generators, demand response by regulating the power consumption of demand-side resources is getting greater attention. On the demand-side, inverter air conditioners (IACs) account for a high power consumption percentage and have huge regulation potential. However, it remains a significant challenge to control large-scale IACs. Traditional control methods only consider active power and do not consider the compressor's complex characteristics combining active and reactive power. To address this issue, this article proposes a two-stage method considering system voltage quality. The first stage is using the photovoltaics' operating reserve for maintaining the system voltage in the safe range. The second stage is under more serious voltage deviations to regulate IACs' active power and reactive power based on model predictive control. Finally, hardware-in-the-loop experiments with realistic IAC are conducted to verify the proposed method. The proposed method improves the voltage fluctuation by 23.45% compared to the traditional method. The experimental results demonstrate that the proposed method can effectively maintain the distribution system's voltage within the allowable range.

**Index Terms**—Demand response, hardware-in-the-loop (HIL), inverter air conditioners (IACs), model predictive control (MPC), voltage regulation.

Received 20 June 2024; accepted 20 September 2024. Date of publication 16 October 2024; date of current version 7 January 2025. This work was supported in part by the National Natural Science Foundation of China under Grant 52407075, in part by the Guangdong Basic and Applied Basic Research Foundation, China under Grant 2024A1515010141, in part by the Science and Technology Development Fund, Macau SAR under Grant 001/2024/SKL and Grant 0117/2022/A3, and in part by the Multi-Year Research Grant—General Research Grant 2024 of University of Macau under Grant MYRG-GRG2024-00112-IOTSC. Paper no. TII-24-3090. (Corresponding author: Hongxun Hui.)

The authors are with the State Key Laboratory of Internet of Things for Smart City and the Department of Electrical and Computer Engineering, University of Macau, Macao 999078, China, and also with the Zhuhai UM Science and Technology Research Institute, Zhuhai 519031, China (e-mail: hongxunhui@um.edu.mo).

Digital Object Identifier 10.1109/TII.2024.3468475

## NOMENCLATURE

### Abbreviation

HIL	Hardware-in-the-loop.
IAC	Inverter air conditioner.
IoT	Internet of Things.
MPC	Model predictive control.
OLTC	On-load tap changer.
PCC	Point of common coupling.
PV	Photovoltaic.
QP	Quadratic programming.
RES	Renewable energy source.
RTDS	Real-Time digital simulator.
R	Resistance.
VVC	Voltage-Var control.
X	Reactance.
R/X	X divided by R ratio.

## I. INTRODUCTION

### A. Background and Motivation

DISTRIBUTED RESs are widely used in modern power systems [1]. Traditional generators (e.g., thermal power plants) are phasing out gradually, while RESs and flexible loads are increasing rapidly [2]. The intermittent and uncertain characteristics of RESs power generation bring many problems [3]. For example, partial shading of PV panels can reduce the power generation [4]. Then, the distribution systems with massive PVs may suffer under-voltage problems during cloud passing periods.

To address the above issue brought by intermittent RESs, more operating reserve resources should be established to enhance the distribution system's voltage quality [5]. Traditional operating reserve resources are the regulation capacity reserved during the construction of RESs [6]. Bruno et al. [7] proposed a closed-loop optimal predictive dispatch method with operating reserve constraints to address the fluctuations brought by the high penetration of RESs. However, these operating reserve resources may not deal with more serious voltage deviations in distribution systems gradually [8]. Moreover, the traditional operating reserve is provided from the generation side, and demand-side resources should be explored to provide operating reserves [9].

## B. Literature Review

With the development of the IoTs, it is possible to monitor and control demand-side resources, called demand response [10]. Demand response can provide regulation capacity to the distribution system by regulating the power consumption of flexible loads [11], such as batteries, electric vehicles, heating, ventilation, and air conditioners [12]. Among various flexible loads, IACs have huge regulation potential due to the large share of power consumption [13]. The frequency of the IACs' compressor is adjustable, which allows the IACs to achieve precise cooling according to the setting temperature [14]. It has been demonstrated that IACs have excellent dynamic response characteristics to improve system flexibility [15]. Hua et al. [16] developed the relationship among the operating state, power, and voltage of air conditioners. They proposed a participation priority algorithm for selecting suitable air conditioners for voltage regulation. Furthermore, Hua et al. [17] demonstrated that IAC can be equated to a thermal battery model to regulate the active power and provide a voltage auxiliary regulation service. Wang et al. [18] utilized the IACs to provide power dispatch services for the power system. A two-layer consensus protocol and the initial values updating scheme are proposed to mitigate the impact of RES fluctuations and load variations in a microgrid. These studies have demonstrated that the aggregated IACs can provide voltage regulation services to the power system. However, it is worth mentioning that the above research mainly focused on changing the active power of IACs to participate in the system voltage regulation. The voltage of the distribution system is also affected by the reactive power of loads [19]. Due to the characteristics of high amount of reactance ( $X$ ) divided by the amount of resistance ( $R$ ) ratios ( $R/X$ ) in distribution systems, the voltage dropout is more significant in the case of fluctuating PV power generation. Therefore, the active and reactive power interactions are more significant [20]. Viriyutsahakul et al. [21] analyzed the inverter and converter designs of IACs to show that IACs can provide reactive power to power systems. Potter et al. [22] analyzed the influence of reactive power on the distribution systems at the macro level but do not give a specific solution. Few studies focus on the coordinate control of both active power and reactive power of IACs on the voltage regulation of distribution systems.

## C. Contributions

To fill the above research gaps, this article aims to coordinate the active power and reactive power of IACs to participate in voltage regulation. MPC is a promising method for converting control problems into optimization problems and obtaining the optimal control strategy [23]. Blum et al. [24] used the MPC for flexible load management in buildings and demonstrate that this method saves 40% of heating, ventilation, and air-conditioning energy in two months. However, they do not consider the voltage regulation. Li et al. [25] used the MPC method successfully to construct a cascade controller for optimal voltage control, while they do not consider the regulation ability of flexible loads. Zhao et al. [26] proposed an MPC-based IAC control method for frequency control and obtain significant results. However, they do not consider the voltage regulation and the experiment uses the simulated IAC. Hence, this article focuses on the MPC-based active and reactive power regulation of realistic IACs for improving voltage quality. The main contributions are as follows.

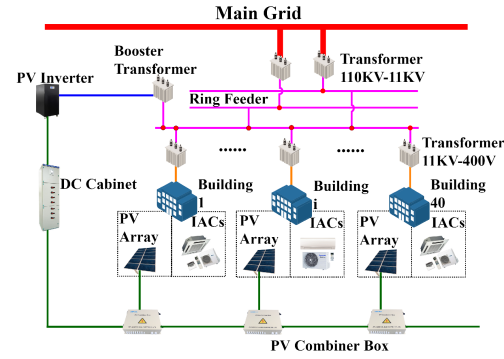


Fig. 1. Typical distribution system structure.

- 1) A two-stage framework is proposed to efficiently coordinate generation-side operating reserves and demand-side resources from the short-term and long-term voltage deviation. The first stage is using the generation-side operating reserves to maintain the system voltage in the safe range, which can quickly respond to the fluctuations of the distribution system voltage. The second stage is using IACs to participate in demand response to realize voltage regulation.
- 2) An MPC-based active and reactive power regulation method is proposed by developing the relationship model between the distribution system's voltage and the IAC compressor's operation characteristics. The characteristics of the high  $R/X$  ratio of the distribution system require better control of reactive power to maintain voltage in the safe range. Previous studies have focused on changing the active power of the IACs without considering the reactive power. Utilizing MPC considering active and reactive power can realize voltage regulation more effectively.
- 3) A RTDS environment with HIL experiments is conducted to verify the proposed method. The realistic IAC is retrofitted to enable remote control and real-time data collection, which allows the IAC to participate conveniently in power system interactions and provide voltage regulation services to the distribution system.

The rest of this article is organized as follows. Section II models the voltage regulation problem. Section III proposes the MPC-based voltage regulation method for the active and reactive power of IACs. Section IV describes the HIL platform. Section V illustrates the experiments and analyzes the results of the experiments. Finally, Section VI concludes this article.

## II. MODELING OF THE VOLTAGE REGULATION IN THE DISTRIBUTION SYSTEM

Fig. 1 shows a typical distribution system structure to address the issue of voltage fluctuations resulting from the cloud shading of the PV panels. This typical distribution system is based on a campus with 40 buildings equipped with some adjustable IACs to participate in the voltage regulation of the distribution system. The PV array is installed on the roof of each building. The PV array on the roof is connected to the dc cabinet through the PV combiner box. Then, the PV power generation is connected to the campus distribution system through a centralized inverter and a booster transformer.

### A. Modeling of PVs

The distribution system's voltage can be influenced by PV because the inverter in the PV power generation module can output reactive power. The reactive power adjustable range of each PV inverter can be described as follows:

$$-\sqrt{(S_{\text{PV}})^2 - (P_{\text{PV}})^2} \leq Q_{\text{PV}} \leq \sqrt{(S_{\text{PV}})^2 - (P_{\text{PV}})^2} \quad (1)$$

where  $Q_{\text{PV}}$  is the reactive power of the PV inverter;  $P_{\text{PV}}$  is the active power of the PV inverter;  $S_{\text{PV}}$  is the capacity of the PV inverter. The active power output of PV power generation is mainly affected by solar insolation and temperature [27]. The active power  $\mathbf{P}_{\text{PVs}}$  and reactive power  $\mathbf{Q}_{\text{PVs}}$  of all the PVs in the campus at time  $t$  can be expressed as follows:

$$\begin{cases} \mathbf{P}_{\text{PVs}}(t) = [P_{\text{PV}}^1(t), P_{\text{PV}}^2(t), \dots, P_{\text{PV}}^{i-1}(t), P_{\text{PV}}^i(t)]^T \\ \mathbf{Q}_{\text{PVs}}(t) = [Q_{\text{PV}}^1(t), Q_{\text{PV}}^2(t), \dots, Q_{\text{PV}}^{i-1}(t), Q_{\text{PV}}^i(t)]^T \end{cases} \quad (2)$$

where  $i$  is the building number,  $\forall i \in \mathcal{I}$ ;  $\mathcal{I}$  is the set of the building.

### B. Modeling of IACs

The state of the IAC involves both active power and reactive power. Altering the setting temperature can influence the state of the IACs, subsequently impacting the active and reactive power to provide voltage regulation for the distribution system [28]. Previous studies have developed operational models of the IAC and thermodynamic models of the corresponding rooms based on first-order ETP models [29]. The thermodynamic process of the room can be expressed as follows:

$$C_{\text{IAC}} \frac{dT_{\text{set}}(t)}{dt} = \frac{T_A(t) - T_{\text{set}}(t)}{R_{\text{IAC}}} - H(t) \quad (3)$$

where  $C_{\text{IAC}}$  is the room's equivalent air heat capacity;  $R_{\text{IAC}}$  is the equivalent thermal resistance of the room's envelope;  $T_{\text{set}}$  is the IAC's setting temperature;  $T_A$  is the room's indoor ambient temperature;  $H$  is the IAC's cooling capacity. The active power consumption and corresponding cooling capacity of the IAC can be expressed as follows:

$$\begin{cases} P_{\text{IAC}}(t) = \kappa_\mu \Delta f_{\text{IAC}} (1 - e^{-t/T_c}) + P_{\text{IAC}}(t-1) \\ H(t) = \kappa_Q \Delta f_{\text{IAC}} (1 - e^{-t/T_c}) + H(t-1) \end{cases} \quad (4)$$

where  $P_{\text{IAC}}$  is the active power of the IAC;  $f_{\text{IAC}}$  is the operating frequency of the IAC;  $\kappa_\mu$  and  $\kappa_Q$  are the constant coefficients of the IAC, respectively;  $T_c$  is the time constant of the IAC's compressor. The reactive power of the IAC correlated with the power factors of the IAC's compressor, which can be expressed as follows:

$$Q_{\text{IAC}}(t) = \sqrt{\left(\frac{P_{\text{IAC}}(t)}{\cos \phi}\right)^2 - (P_{\text{IAC}}(t))^2} \quad (5)$$

where  $Q_{\text{IAC}}$  is the reactive power of the IAC;  $\phi$  is the phase deviation between the voltage and current of the IAC;  $\cos \phi$  is the power factor of the IAC. When the setting temperature of IAC at time  $t$  is  $T_{\text{set}}$ , the active power and reactive power consumption of the IACs are deterministic, as follows:

$$\begin{cases} P_{\text{IAC}}^{i,j}(t) = f_P(T_{\text{set}}^{i,j}(t)) \\ Q_{\text{IAC}}^{i,j}(t) = f_Q(T_{\text{set}}^{i,j}(t), \cos \phi(t)) \end{cases} \quad (6)$$

where  $j$  is the IAC number in each building,  $\forall j \in \mathcal{J}$ ;  $\mathcal{J} = [1, 2, 3, \dots, J-1, J]$  is the sets of IAC in each building;  $J$  is

the total number of IACs in each building. The active power  $\mathbf{P}_{\text{IACs}}$  and reactive power  $\mathbf{Q}_{\text{IACs}}$  of all the IACs in the campus at time  $t$  can be expressed as follows:

$$\begin{cases} \mathbf{P}_{\text{IACs}}(t) = [\sum_{j \in \mathcal{J}} P_{\text{IAC}}^{1,j}(t), \sum_{j \in \mathcal{J}} P_{\text{IAC}}^{2,j}(t), \dots, \sum_{j \in \mathcal{J}} P_{\text{IAC}}^{i,j}(t)]^T \\ \mathbf{Q}_{\text{IACs}}(t) = [\sum_{j \in \mathcal{J}} Q_{\text{IAC}}^{1,j}(t), \sum_{j \in \mathcal{J}} Q_{\text{IAC}}^{2,j}(t), \dots, \sum_{j \in \mathcal{J}} Q_{\text{IAC}}^{i,j}(t)]^T \end{cases} \quad (7)$$

### C. Modeling of Voltage Regulation in Distribution Systems

The distribution system voltage is directly influenced by the active and reactive power of loads. If the power supply of generating units is not balanced with the power consumption of the loads, the voltage of the distribution system will exceed the safety range. The relationship between voltage and power is based on the voltage sensitivity matrix [30], which is expressed as follows:

$$\begin{bmatrix} \Delta \theta \\ \Delta \mathbf{V} \end{bmatrix} = \mathbf{J}^{-1} \begin{bmatrix} \Delta \mathbf{P} \\ \Delta \mathbf{Q} \end{bmatrix} = \begin{bmatrix} \mathbf{S}_{P\theta} & \mathbf{S}_{Q\theta} \\ \mathbf{S}_{PU} & \mathbf{S}_{QU} \end{bmatrix} \begin{bmatrix} \Delta \mathbf{P} \\ \Delta \mathbf{Q} \end{bmatrix} \quad (8)$$

where  $\theta$  is the phase angle at each node in the system;  $\mathbf{V}$  is the voltage at each node in the system;  $\Delta \mathbf{P}$  and  $\Delta \mathbf{Q}$  are the deviations of active power and reactive power at each node in the system, respectively;  $\mathbf{J}$  is the jacobian matrix;  $\mathbf{S}_{P\theta}$  and  $\mathbf{S}_{Q\theta}$  are the phase angle sensitivity of active power and reactive power, respectively;  $\mathbf{S}_{PU}$  and  $\mathbf{S}_{QU}$  are the voltage sensitivity of active power and reactive power, respectively.

The active and reactive power in the distribution system is correlated with the main grid, loads, and PVs, which can be expressed as follows:

$$\begin{cases} \mathbf{P}(t) = \mathbf{P}_{\text{main}}(t) + \mathbf{P}_{\text{PVs}}(t) - \mathbf{P}_{\text{loads}}(t) \\ \mathbf{Q}(t) = \mathbf{Q}_{\text{main}}(t) + \mathbf{Q}_{\text{PVs}}(t) - \mathbf{Q}_{\text{loads}}(t) \end{cases} \quad (9)$$

where  $\mathbf{P}_{\text{main}}$  and  $\mathbf{Q}_{\text{main}}$  are the active power and reactive power support by main grid, respectively;  $\mathbf{P}_{\text{loads}}$  and  $\mathbf{Q}_{\text{loads}}$  are the active power and reactive power of all the demand-side resources in the system, respectively. Assuming that the IACs of demand-side resources can participate in the voltage regulation for the above disturbance at time  $t$ . Here, we separate the active load power  $\mathbf{P}_{\text{loads}}$  and reactive load power  $\mathbf{Q}_{\text{loads}}$  into two parts. The first part is controllable part  $\mathbf{P}_{\text{IACs}}$  and  $\mathbf{Q}_{\text{IACs}}$ . This part can be adjusted by adjusting the active power and reactive power of IACs. The second part is noncontrollable loads. It is assumed that the disturbance is from the fluctuating output power of PVs due to the variable environment. The available regulation resources are from PVs and IACs, which can be expressed as follows:

$$\begin{cases} \mathbf{P}_{\text{reg}}(t) = \mathbf{P}_{\text{PVs}}^{\text{reg}}(t) + \mathbf{P}_{\text{IACs}}^{\text{reg}}(t) \\ \mathbf{Q}_{\text{reg}}(t) = \mathbf{Q}_{\text{PVs}}^{\text{reg}}(t) + \mathbf{Q}_{\text{IACs}}^{\text{reg}}(t) \end{cases} \quad (10)$$

where  $\mathbf{P}_{\text{reg}}$  and  $\mathbf{Q}_{\text{reg}}$  are the active and reactive power support by regulation resources, respectively;  $\mathbf{P}_{\text{PVs}}^{\text{reg}}$  and  $\mathbf{Q}_{\text{PVs}}^{\text{reg}}$  are the available active power and reactive power from PVs for providing operating reserve, respectively;  $\mathbf{P}_{\text{IACs}}^{\text{reg}}$  and  $\mathbf{Q}_{\text{IACs}}^{\text{reg}}$  are the available active power and reactive power from IACs, respectively. In this study, the voltage regulation problem is how to regulate the active power and reactive power of the regulation resources in the system to reduce the voltage deviation caused by the cloud shading of PV panels. The voltage variation from the regulation

resources can be expressed as follows:

$$\Delta \mathbf{V}(t) = [\mathbf{V}(t+1)] - [\mathbf{V}(t)] = [\mathbf{S}_{\text{PU}} \quad \mathbf{S}_{\text{QU}}] \begin{bmatrix} \mathbf{P}_{\text{reg}}(t) \\ \mathbf{Q}_{\text{reg}}(t) \end{bmatrix} \quad (11)$$

which can be rewritten as follows:

$$[\mathbf{V}(t+1)] = [\mathbf{V}(t)] + [\mathbf{S}_{\text{PU}} \quad \mathbf{S}_{\text{QU}}] \begin{bmatrix} \mathbf{P}_{\text{reg}}(t) \\ \mathbf{Q}_{\text{reg}}(t) \end{bmatrix}. \quad (12)$$

Denote the system's state (i.e., the distribution system voltage) as  $\mathbf{x}$  and control input (i.e., the regulation resources) as  $\mathbf{u}$ . The relationship between the  $\mathbf{x}$  and  $\mathbf{u}$  can be expressed as follows:

$$\mathbf{x}(t+1) = \mathbf{Ax}(t) + \mathbf{Bu}(t) \quad (13)$$

where

$$\begin{cases} \mathbf{x}(t) = \mathbf{V}(t) \\ \mathbf{A} = \mathbf{I} \\ \mathbf{B} = [\mathbf{S}_{\text{PU}} \quad \mathbf{S}_{\text{QU}}] \\ \mathbf{u}(t) = \begin{bmatrix} \mathbf{P}_{\text{reg}}(t) \\ \mathbf{Q}_{\text{reg}}(t) \end{bmatrix} \end{cases} \quad (14)$$

where  $\mathbf{I}$  is the unitary matrix;  $\mathbf{x}(t+1)$  and  $\mathbf{x}(t)$  are the voltage at time  $t+1$  and  $t$ , respectively.

### III. MPC-BASED VOLTAGE REGULATION METHOD

#### A. Two-Stage Collaborative Method

This article proposes a two-stage collaborative method to realize the voltage regulation for under-voltage problems. The two-stage collaborative method is designed from the short-term voltage deviation and long-term voltage deviation aspect. The two-stage coordinated scheduling approach allows for the utilization of generation-side operating reserves and reduces the demand-side resources to be dispatched. This approach provides users with better comfort in using IACs. The equation for the voltage regulation method is as follows:

$$S_{\text{system}}(t) = \begin{cases} S_{\text{stage1}}(t), & \mathbf{P}_{\text{PVs}}^{\text{env}}(t) \leq \mathbf{P}_{\text{PVs}}^{\text{reg}}(t) \\ & \& \mathbf{Q}_{\text{PVs}}^{\text{env}}(t) \leq \mathbf{Q}_{\text{PVs}}^{\text{reg}}(t) \\ S_{\text{stage2}}(t), & \text{other} \end{cases} \quad (15)$$

where  $S_{\text{system}}(t)$  is the regulation stage at the time  $t$ ;  $S_{\text{stage1}}(t)$  is the first regulation stage at the time  $t$ ;  $S_{\text{stage2}}(t)$  is the second regulation stage at the time  $t$ ;  $\mathbf{P}_{\text{PVs}}^{\text{env}}$  and  $\mathbf{Q}_{\text{PVs}}^{\text{env}}$  are the fluctuating output power of PVs due to variable environment, respectively.

In the first stage, we use the operating reserve from PVs to maintain the voltage in the safe range. This stage can quickly respond to the fluctuations of the distribution system and stabilize the distribution system voltage on the power generation side. The system will launch the second stage of control if the PVs' operating reserve still cannot maintain the system voltage in the safe range. The second stage uses the MPC algorithm to design a power continuous adjustment controller, allowing for up or down the active power and reactive power adjustments. This coordination considers minimizing both short-term and long-term voltage deviations. The two-stage collaborative method provides a flexible and adaptive framework that can accommodate varying power system conditions and user preferences. It allows the system to provide a balance between voltage security, efficiency, and user satisfaction.

#### B. MPC Controller

The basic idea of the MPC controller is to solve the optimization problem at each time slot to obtain the optimal control instruction over the next finite time horizon [31]. Equation (13) is the system state function of the voltage regulation problem. From (10), it can be known that regulation resources include PV operating reserves and IACs. The PV operating reserve has already been utilized in the first stage. Therefore, the control input in the second stage is the active and reactive power of the IACs. The MPC controller can control the active and reactive power of the IACs synchronously, considering the active and reactive power interactions, to optimally balance the power demand and voltage security of the distribution system with the characteristics of high  $R/X$  ratios. Fig. 2 shows the architecture of the MPC controller. The MPC controller consists of constraints, the predictive model, cost function, and optimizer [32].

**a) Constraints:** The constraints on inputs  $\mathbf{u}$  and system state  $\mathbf{x}$  are set based on the rated power of the IACs, which can be expressed as follows:

$$\begin{cases} 0 \leq \mathbf{u}(t+l) \leq \mathbf{u}_{\max} \\ \mathbf{x}_{\min} \leq \mathbf{x}(t+l) \leq \mathbf{x}_{\max} \end{cases} \quad (16)$$

where  $\mathbf{u}_{\max}$  is the maximum operating power of IACs;  $\mathbf{x}_{\min}$  and  $\mathbf{x}_{\max}$  are the minimum and maximum operating voltage of the distribution system voltage, respectively;  $l \in \mathcal{L}; \mathcal{L} = [1, 2, \dots, m]$ . The constraints ensure that the control strategy operates within the practical operational range of the IACs and helps to reduce the voltage fluctuations in the distribution system.

**b) Predictive Model:** Let  $\mathbf{u}(t+m|t)$  denote the predicted control input of the step  $t+m$  at moment  $t$ . To allow the MPC controller to update the control strategy more efficiently within each prediction step, it is necessary to define the control horizon  $n$  to be less than or equal to the prediction horizon  $m$ . Therefore, the control input of the system varies in  $n$  steps from moment  $t$  and remains constant after moment  $t+n$ , which can be expressed as follows:

$$\mathbf{u}(t+l|t) = \begin{cases} \mathbf{u}(t+l|t), & l \leq n \\ \mathbf{u}(t+n|t), & l > n. \end{cases} \quad (17)$$

Let  $\mathbf{x}(t+m|t)$  denote the predicted system state of the step  $t+m$  at moment  $t$ . The predictive model from moment  $t$  to the moment  $t+m$  can be expressed as follows:

$$\begin{cases} \mathbf{x}(t|t) = \mathbf{x}(t) \\ \mathbf{x}(t+1|t) = \mathbf{Ax}(t|t) + \mathbf{Bu}(t|t) \\ \mathbf{x}(t+2|t) = \mathbf{A}^2\mathbf{x}(t|t) + \mathbf{ABu}(t|t) + \mathbf{Bu}(t+1|t) \\ \mathbf{x}(t+3|t) = \mathbf{A}^3\mathbf{x}(t|t) + \mathbf{A}^2\mathbf{Bu}(t|t) + \mathbf{ABu}(t+1|t) \\ & + \mathbf{Bu}(t+2|t) \\ & \dots \\ \mathbf{x}(t+m|t) = \mathbf{A}^m\mathbf{x}(t|t) + \mathbf{A}^{m-1}\mathbf{Bu}(t|t) + \dots \\ & + \mathbf{A}^{m-l}\mathbf{Bu}(t+l+1|t) + \dots \\ & + \mathbf{Bu}(t+m-1|t). \end{cases} \quad (18)$$

The above equations can be expressed as a matrix as follows:

$$\mathbf{X} = \alpha \mathbf{x}(t|t) + \beta \mathbf{U} \quad (19)$$

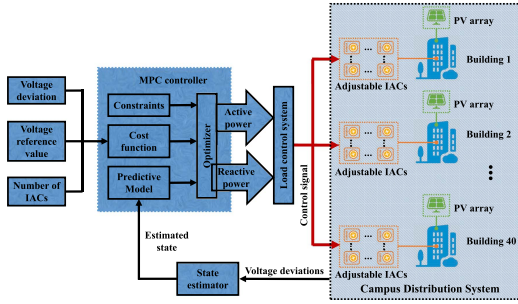


Fig. 2. Architecture of the MPC controller.

where

$$\left\{ \begin{array}{l} \mathbf{X} = [\mathbf{x}(t|t) \quad \mathbf{x}(t+1|t) \quad \dots \quad \mathbf{x}(t+m|t)]^T \\ \mathbf{U} = [\mathbf{u}(t|t) \quad \mathbf{u}(t+1|t) \quad \dots \quad \mathbf{u}(t+m-1|t)]^T \\ \boldsymbol{\alpha} = [\mathbf{I} \quad \mathbf{A} \quad \mathbf{A}^2 \quad \mathbf{A}^3 \quad \dots \quad \mathbf{A}^m]^T \\ \boldsymbol{\beta} = \begin{bmatrix} \mathbf{0} & \mathbf{0} & \dots & \mathbf{0} \\ \mathbf{B} & \mathbf{0} & \dots & \mathbf{0} \\ \mathbf{AB} & \mathbf{B} & \dots & \mathbf{0} \\ \dots & \dots & \dots & \dots \\ \mathbf{A}^{m-1}\mathbf{B} & \mathbf{A}^{m-2}\mathbf{B} & \dots & \mathbf{B} \end{bmatrix}. \end{array} \right. \quad (20)$$

*c) Cost Function:* The cost function of the MPC controller is considered from three objectives: system security, control cost, and control performance.

The security objective of the MPC controller is to maintain the voltage in a safe range, which can be expressed as follows:

$$\min(\mathbf{V}(t) - \mathbf{V}_{\text{ref}}(t)) \quad (21)$$

where  $\mathbf{V}_{\text{ref}}$  is the reference voltage of the distribution system. Let  $\mathbf{V}_{\text{ref}}(t+m|t)$  denote the predicted reference voltage of the step  $t+m$  at moment  $t$ . The reference voltage of the system from moment  $t$  to the moment  $t+m$  can be expressed as follows:

$$\bar{\mathbf{X}} = [\mathbf{V}_{\text{ref}}(t|t) \quad \mathbf{V}_{\text{ref}}(t+1|t) \quad \dots \quad \mathbf{V}_{\text{ref}}(t+m|t)]^T. \quad (22)$$

Therefore, the security objective from moment  $t$  to the moment  $t+m$  can be expressed as follows:

$$\begin{aligned} \mathbf{E} &= \mathbf{X} - \bar{\mathbf{X}} \\ &= [\mathbf{V}(t|t) - \mathbf{V}_{\text{ref}}(t|t) \quad \mathbf{V}(t+1|t) - \mathbf{V}_{\text{ref}}(t+1|t) \\ &\quad \dots \quad \mathbf{V}(t+m|t) - \mathbf{V}_{\text{ref}}(t+m|t)]. \end{aligned} \quad (23)$$

The cost function for the security objective can be expressed as follows:

$$\min f_1 = \min(\mathbf{E}^T \mathbf{W} \mathbf{E}) \quad (24)$$

where the  $\mathbf{W}$  value implies the weight of the safety objective to be considered in the MPC controller optimization.

The high R/X ratio feature of the distribution system leads to high line active power losses [33]. Therefore, it is necessary to consider the control cost of the MPC controller. The cost function for the control cost objective can be expressed as follows:

$$\min f_2 = \min(\mathbf{U}^T \mathbf{R} \mathbf{U}) \quad (25)$$

where the  $\mathbf{R}$  value implies the weight of the control cost to be considered in the MPC controller optimization.

The terminal error  $\mathbf{E}_m$  is an important metric for control the performance of an MPC controller, which can be expressed as

follows:

$$\min f_3 = \min(\mathbf{E}_m^T \mathbf{F} \mathbf{E}_m) \quad (26)$$

where

$$\mathbf{E}_m = \mathbf{V}(t+m|t) - \mathbf{V}_{\text{ref}}(t+m|t) \quad (27)$$

where the  $\mathbf{F}$  value implies the weight of the control performance to be considered in the MPC controller optimization;  $\mathbf{V}(t+m|t)$  is the predicted system voltage of the step  $t+m$  at moment  $t$ ;  $\mathbf{V}_{\text{ref}}(t+m|t)$  is the predicted reference voltage of the step  $t+m$  at moment  $t$ . Terminal error refers to the difference between the system's state  $\mathbf{V}(t+m|t)$  and the desired target state  $\mathbf{V}_{\text{ref}}(t+m|t)$  at the last time step  $m$  of the prediction horizon. Minimizing this error helps the system to better achieve and maintain the target state.

From the above analysis, we can obtain the cost function of MPC controller as follows:

$$\begin{aligned} \min \mathbf{J}_{\text{mpc}} &= \min(f_1 + f_2 + f_3) \\ &= \min(\mathbf{E}^T \mathbf{W} \mathbf{E} + \mathbf{U}^T \mathbf{R} \mathbf{U} + \mathbf{E}_m^T \mathbf{F} \mathbf{E}_m). \end{aligned} \quad (28)$$

*d) Optimizer:* QP is a mathematical optimization technique that finds the optimal solution to a quadratic objective function, subject to linear constraints. Through the QP algorithm, we can obtain the optimal control sequences  $\{\mathbf{u}^{\text{opt}}(t), \mathbf{u}^{\text{opt}}(t+1), \dots, \mathbf{u}^{\text{opt}}(t+m-1)\}$  over the next finite time horizon. The first control  $\mathbf{u}^{\text{opt}}(t)$  is applied to the system, and the process is repeated at the next period. This process is referred to as rolling optimization. The rolling optimization allows the MPC controller to adjust the control input based on the current state of the system and the predicted future behaviors [34]. The rolling optimization feature can avoid some uncertain factors. For example, the user of the IACs modifies the setting temperatures of the IACs on the demand side, causing the IACs not to respond to the control commands from the MPC controller. The rolling optimization feature of the MPC can compensate for the error in the next period. Furthermore, in a high R/X ratio distribution system, the prediction of load control is beneficial for stabilizing voltage and optimizing power allocation. MPC can provide a faster response with instantaneous prediction and control to mitigate transient problems in the system. The flowchart of the voltage regulation process is shown in Fig. 3.

#### IV. HIL PLATFORM DEVELOPMENT

HIL involves integrating real hardware components into a simulated environment to test the performance and functionality of a system [35]. The platform consists of RTDS environment, load control system, sensors, communication modules, controllers, and realistic IACs. Fig. 4 shows the framework of the HIL platform.

##### A. Real-Time Digital Simulator

Since verifying the proposed method directly on the physical distribution system may be challenging and unsafe, we simulate the power distribution system in RTDS. RTDS is a powerful power system simulator that has been highly approved. Its simulation outcomes are trustable compared to the real world. The simulation uses RTDS software on a computer with a central processing unit of Intel(R) Core(TM) i7-8700 @ 3.20 GHz and 16 GB memory. This study adopts a campus distribution

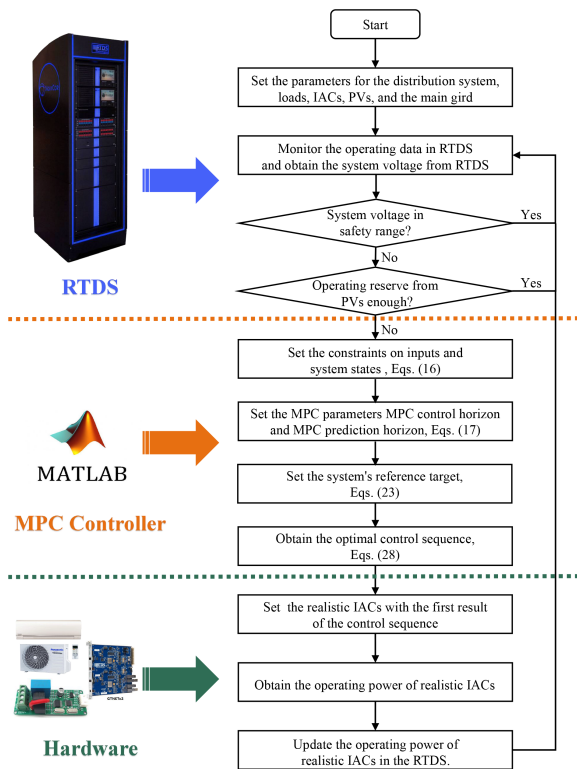


Fig. 3. Two-stage collaborative method.

system with 40 buildings, as shown in Fig. 5, to validate the effectiveness of the proposed collaborative algorithm. RSCAD FX and RUNTIME are the RTDS software. We design the schematic of the campus distribution system with RSCAD FX and run it on the RTDS device. RUNTIME allows us to implement parameters for observing the operation of the grid. GTNET is the component of RTDS, which can input parameters (i.e., load parameters of each node, solar insolation of PV panels, generator parameters, etc.) from the computer to the RTDS device. It also can receive the operation status (i.e., voltage, active power, reactive power, etc.) from the RTDS device to the computer.

### B. Load Control System

This study uses realistic IACs to do the HIL voltage regulation experiment in a campus distribution system based on the RTDS environment and load control system. The model of IACs used in the experiment is Daikin KFR-36W/BP. The IACs should be modified to enable the remote control and real-time data collection of the power parameters. A load control system is developed based on the microcontroller ESP32, which has Bluetooth and Wi-Fi functions on board [36]. The microcontroller communicates with the computer through Wi-Fi. The power module collects the power operation parameters of the IACs and transmits them to the microcontroller via 485 wired transmission. The microcontroller receives control commands from the computer and controls the IACs through the infrared remote control module.

The load control system is constructed in the laboratory, as shown in Fig. 6. The infrared sensor can remotely control the IACs, and the sensor in the load control system can monitor the power parameters. Through the communication modules in the load control system, we can realize the real-time interaction of IACs with the RTDS and MPC controller.

TABLE I  
SOLAR INSOLATION CONDITIONS IN DIFFERENT SCENARIOS

	Scenario 1	Scenario 2	Scenario 3
Start insolation	1000W/m <sup>2</sup>	1000W/m <sup>2</sup>	1000W/m <sup>2</sup>
Stop insolation	100W/m <sup>2</sup>	100W/m <sup>2</sup>	100W/m <sup>2</sup>
Time	125S	200S	250S

TABLE II  
CONTROL METHODS IN DIFFERENT CASES

Case 0	Without regulation
Case 1	With operating reserve from PVs
Case 2	Stage 1: With operating reserve from PVs Stage 2: MPC without considering the reactive power regulation
Case 3 (Proposed)	Stage 1: With operating reserve from PVs Stage 2: MPC with considering the reactive power regulation

### C. MPC Controller

The MPC controller is realized on the computer through MATLAB software. The MPC controller can monitor the real-time operating power of the IACs from the load control system and the system voltage deviations from the RTDS device. Then, the MPC controller processes and sends regulation signals to the IACs. The IACs will change their operating states according to the signals sent by the controller to realize the regulation of active and reactive power. Next, the load control system transmits active and reactive power variation to RTDS devices in real-time. Finally, the MPC controller will conduct the next round of rolling control based on the variation of the distribution system.

## V. CASE STUDY AND EXPERIMENT

### A. Experiment Setup

The experiment simulates the situation in which the clouds pass through the PV panels, causing a voltage drop in the distribution system. The allowable voltage fluctuation range in the experiments is set to [0.95, 1.05] p.u.. There are 500 adjustable IACs designed in each building in the campus distribution system. Each building can provide around 0.6 MW of active power and 0.125 Mvar of reactive power regulation capacity. The total IAC power of all buildings is around 24 MW active power and 5 Mvar reactive power. Table I shows three conditions of the clouds shading the PV panels. Fig. 7 shows the results without voltage regulation resources. Fig. 7(a) shows the variation curves of insolation bias in different scenarios. Fig. 7(b) shows the variation curves of voltage at the PCC. Fig. 7(c) shows the voltage variation at each node in scenario 3. The experimental results in Fig. 7 show that the variation of solar insolation in different scenarios leads to under-voltage problems in the distribution system. In all the scenarios 1–3, the distribution system voltage exceeds the limit, and the voltage quality worsens. The following section will compare different voltage regulation methods in Table II.

### B. Voltage Regulation Result Analysis

Fig. 8 shows the results using different voltage regulation methods in three scenarios of clouds passing through the PV panels. By comparing Case 0 and Case 1, it can be seen that the voltage does not drop rapidly at the beginning when the clouds pass through the PV panels in Case 1. However, when the PV power generation capacity decreases to a certain level (i.e., the

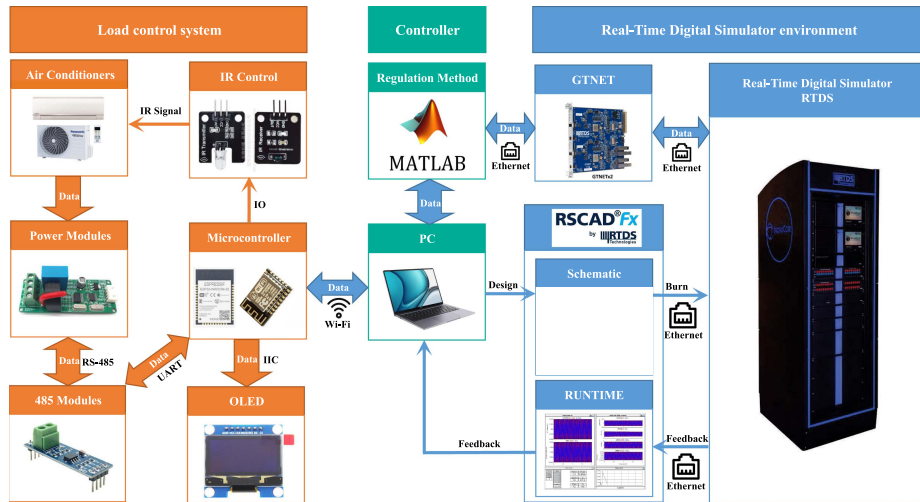


Fig. 4. Environment platform based on RTDS and HIL.

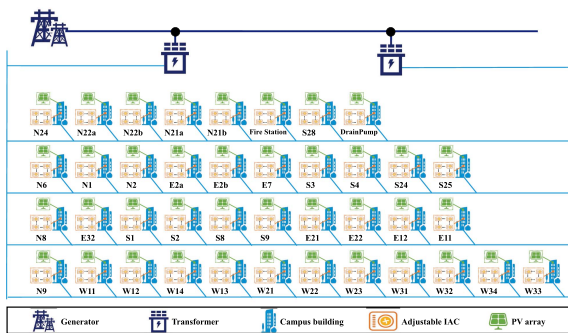


Fig. 5. Campus distribution system with 40 buildings.

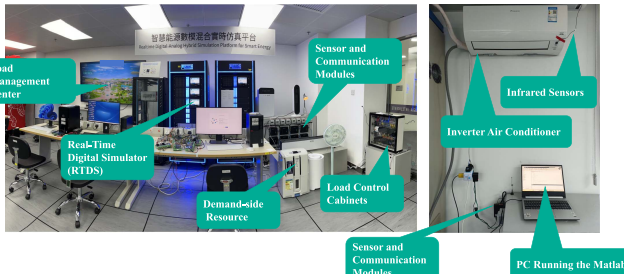


Fig. 6. Field demonstration of the load control system for IACs to be remote control and real-time data collection of the power parameters.

insolation decreases to  $750 \text{ W/m}^2$ ), the power system voltage will decrease quickly and drop below the security voltage range. The operating reserve cannot maintain the voltage security of the distribution system in this situation. Nevertheless, the operating reserve in Case 1 can reduce voltage deviation nadir value from  $3.41 \times 10^{-3}$  p.u. to  $3.04 \times 10^{-3}$  p.u., which is reduced by around 10.85%. The operating reserve from PVs can only deal with short-term or minor voltage deviations. However, it cannot maintain the system voltage within the safety range under long-term or more serious voltage deviations.

Compared with the method in Case 1, Case 2, and Case 3 consider the two-stage collaborative method, as shown in Table II. Similar to most previous methods, the MPC controller of Case 2 only considers the active power regulation of the

IACs, and the IACs' reactive power is set as a fixed factor binding it to the active power. The MPC controller of Case 3 considers the active and reactive power of the IACs in the voltage regulation process. By comparing Case 0 and Case 2, it can be seen that the method in Case 2 can reduce voltage fluctuations from  $3.41 \times 10^{-3}$  p.u. to  $0.8 \times 10^{-3}$  p.u., which reduces around 76.54%. From the comparison of Cases 0 and 3, it can be seen that Case 3 almost has no voltage deviations, though there are still tiny fluctuations. It can also be seen that Case 3 is effective in maintaining the system voltage at normal levels in all three scenarios. Therefore, the system changed to the second stage to maintain system voltage within the safe range. The second stage is using IACs to participate in demand response to realize voltage regulation. The IACs' active and reactive power can be regulated based on MPC to minimize the long-term voltage deviations.

To better analyze the proposed method's effectiveness, we illustrate each node's voltage variation and the voltage bias in Scenario 3, as shown in Fig. 9. It can be seen that both the Case 2 and Case 3 methods can improve the distribution system voltage quality. However, the voltage deviations of nodes {3, 4, 5, 6, 7} in Case 2 still exceed the limit and suffer from under-voltage problems, as shown in Fig. 9(b). According to this result, it is not easy to maintain the system voltage to the original state only considering the active power of the IAC. By contrast, as shown in Fig. 9(c) and (f), all the nodes' voltage can be maintained in the required limit range by considering both active power and reactive power of IACs. It proves that the proposed method in this study can effectively mitigate voltage fluctuations and improve the voltage quality.

### C. Sampling Time Period for the Control System

The RTDS can realize continuous real-time distribution system simulation with a  $50\text{--}65 \mu\text{s}$  simulation time step. The control system can collect the status of the distribution system from RTDS and realize the control algorithm accordingly in each sampling period. The experiments for Case 3 with different sampling period settings (i.e., Table III) are shown in Fig. 10(a). Different sampling periods for the control system will obtain different control results. Sampling periods of 1 s and 5 s for the control system lead to  $1.2707 \times 10^{-4}$  and  $9.687 \times 10^{-4}$  voltage

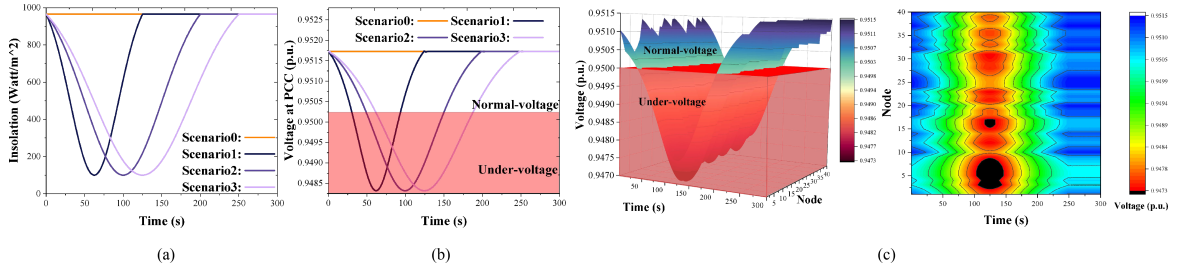


**Fig. 7.** Experiment results of clouds passing through the PV panels causing the distribution system's voltage drop. (a) Insolation bias. (b) Voltage deviations at PCC. (c) Voltage deviations at each node in Scenario 3.

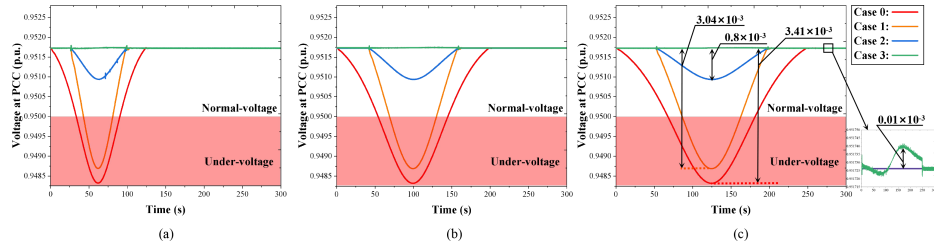


**Fig. 8.** Results using different voltage regulation methods in three scenarios. (a) Scenario 1. (b) Scenario 2. (c) Scenario 3.

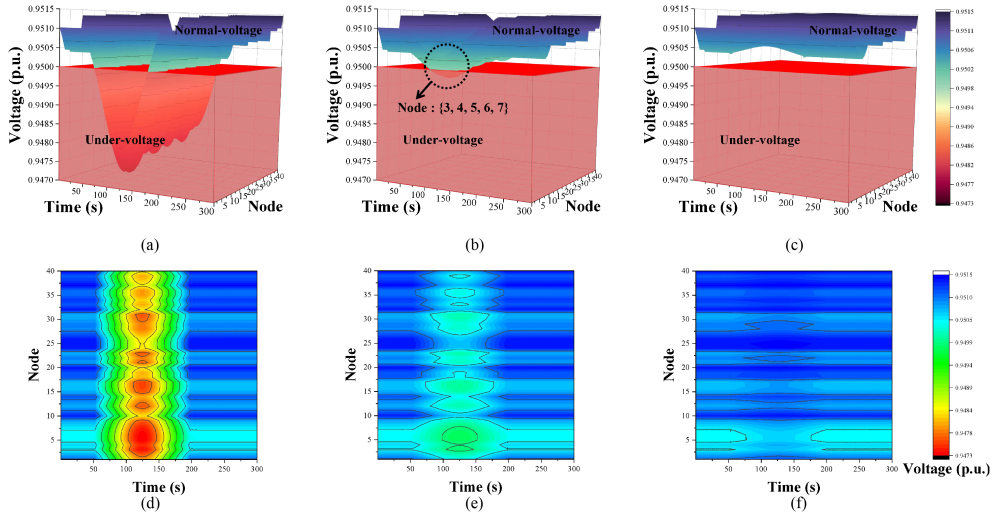


**Fig. 9.** Voltage variation and the voltage bias of each node in scenario 3. (a) Voltage variation in Case 1. (b) Voltage variation in Case 2. (c) Voltage variation in Case 3. (d) Voltage bias in Case 1. (e) Voltage bias in Case 2. (f) Voltage bias in Case 3.

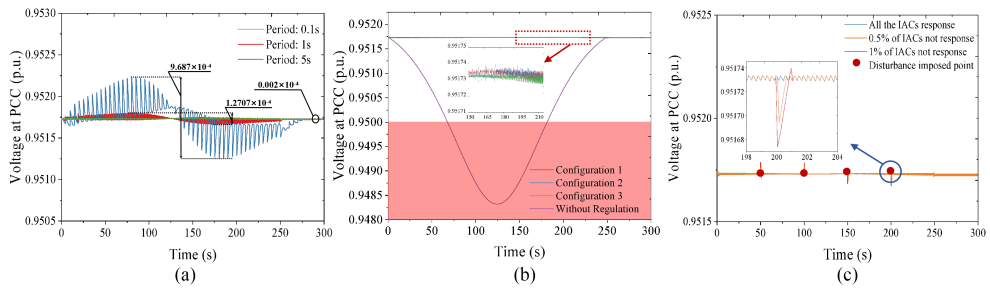


**Fig. 10.** Result for the influence of sampling time, MPC parameter configurations, and uncertainty factors in Case 3. (a) Different sampling time period settings for the control system in Case 3. (b) Different control and prediction horizon for MPC algorithm in Case 3. (c) Uncertainty factor imposed in Case 3.

**TABLE III**  
DIFFERENT SAMPLING TIME PERIOD SETTING FOR THE CONTROL SYSTEM

	<i>Period 1</i>	<i>Period 2</i>	<i>Period 3</i>
Time	0.1s	1s	5s

**TABLE IV**  
PROCESSING TIME OF MPC ALGORITHM UNDER DIFFERENT PREDICTION AND CONTROL HORIZONS

Configuration	<i>1</i>	<i>2</i>	<i>3</i>
Control horizons	5	5	5
Prediction horizons	5	10	20
Iterations	3000	3000	3000
Processing speed	0.1002s	0.1685s	0.1919s

amplitudes in the system, respectively. Therefore, it is more suitable to set 0.1 s as the sampling period for the control system.

#### D. Selection of Control and Prediction Horizons

The experimental result of the processing time of the proposed algorithm under different control and prediction horizons are shown in Table IV. As shown in Fig. 10(b), the proposed MPC-based voltage regulation algorithm with different control and prediction horizons in Case 3 can reach similar processing results, while the processing speed is faster with a smaller prediction horizon. Therefore, the control and prediction horizons for this experiment are set to be 5.

#### E. Uncertain Factors for the Control System

Uncertain factors, such as user behaviors, can affect the effectiveness of the IAC response to control commands from the MPC controller. Fig. 10(c) shows the voltage regulation result of 0.5% (i.e., 100) and 1% (i.e., 200) IACs not responding to the control commands sent by the MPC controller. It can be seen that the voltage fluctuates slightly at the point where the disturbance is imposed. The MPC controller can periodically adjust the control input based on the current state of the system and the predicted future behaviors. Therefore, these slight fluctuations are quickly smoothed out due to the rolling optimization feature of the MPC controller, which can quickly predict and correct them.

## VI. CONCLUSION

The distribution system is facing more voltage fluctuation problems due to the high penetration of renewable resources. More seriously, the distribution systems with massive local PV generation may suffer under-voltage problems during cloud passing periods. This article proposes a voltage regulation method to cope with the under-voltage problems. The first stage uses the operating reserve of PVs for maintaining the system's voltage in the safe range. The HIL experiments show that operating reserves can reduce voltage fluctuations by around 10.85%. The second stage is using IACs to participate in demand response to realize voltage regulation. The IACs control scheme is designed to regular the active power and reactive power based on MPC while minimizing the long-term voltage deviations. Compared with traditional methods only considering active power regulation of IACs, the proposed method can reduce voltage fluctuations from  $0.8 \times 10^{-3}$  p.u. to  $0.01 \times 10^{-3}$  p.u. The HIL experiment platform with RTDS proves that our proposed method can effectively improve the voltage quality of distribution systems.

## APPENDIX A PROOF OF THE MPC CONVERGENCE

Equation (28) is the objective cost function of MPC optimization processing, which can be represented as

$$\mathbf{J}_{\text{opt}}(t) = \sum_{l=1}^m \varsigma(\hat{\mathbf{E}}_l(t+l|t), \hat{\mathbf{u}}(t+l-1|t)) \quad (29)$$

where

$$\hat{\mathbf{E}}_l = \hat{\mathbf{V}}(t+l|t) - \hat{\mathbf{V}}_{\text{ref}}(t+l|t) \quad (30)$$

where  $\hat{\mathbf{V}}(t+l|t)$  is the predicted system voltage of the step  $t+l$  at moment  $t$ ;  $\hat{\mathbf{V}}_{\text{ref}}(t+l|t)$  is the predicted reference voltage of the step  $t+l$  at moment  $t$ ;  $\hat{\mathbf{u}}(t+l-1|t)$  are the predicted control inputs of the step  $t+l-1$  at moment  $t$ .

The Lyapunov stability proof can be used to verify the convergence of the MPC. Consider the optimal value obtained from the objective function of the MPC controller for each period. The optimal value for each period  $\mathbf{J}_{\text{opt}}^0(t)$  is defined as the Lyapunov function. From (29), we can obtain the relationship as follows:

$$\begin{cases} \varsigma(\mathbf{E}_l, \mathbf{u}) = 0, \mathbf{E}_l = 0, \mathbf{u} = 0 \\ \varsigma(\mathbf{E}_l, \mathbf{u}) > 0, \text{ otherwise.} \end{cases} \quad (31)$$

Assume that  $\mathbf{E}_l = 0$  and  $\mathbf{u} = 0$  are an equilibrium state of the system, i.e.,  $\varsigma(0, 0) = 0$ . If each period of optimization has a feasible solution  $\mathbf{u}^{\text{opt}}(t+l)$  and can be solved to obtain the global optimization, the system is stable at  $\mathbf{E}_l = 0$  and  $\mathbf{u} = 0$ . Therefore, the Lyapunov function  $\mathbf{J}_{\text{opt}}^0(t)$  has positive definiteness.

Assume that the system model is unbiased and does not take into account the interference of noise. The predicted state of the system is the same as its actual state, which can be expressed as follows:

$$\begin{cases} \mathbf{E}_l(t+l) = \hat{\mathbf{E}}_l(t+l|t) \\ \mathbf{u}_l(t+l) = \hat{\mathbf{u}}_l(t+l|t). \end{cases} \quad (32)$$

Therefore

$$\begin{aligned} \mathbf{J}_{\text{opt}}^0(t+1) &= \min \sum_{l=1}^m \varsigma(\mathbf{E}_{l+1}(t+l+1|t), \mathbf{u}(t+l|t)) \\ &= \min \left\{ \sum_{l=1}^m \varsigma(\mathbf{E}_l(t+l|t), \mathbf{u}(t+l-1|t)) \right. \\ &\quad \left. - \varsigma(\mathbf{E}_1(t+1|t), \mathbf{u}(t|t)) \right. \\ &\quad \left. + \varsigma(\mathbf{E}_m, \mathbf{u}(t+m-1|t)) \right\} \\ &= -\varsigma(\mathbf{E}_1(t+1|t), \mathbf{u}(t|t)) \\ &\quad + \min \left\{ \sum_{l=1}^m \varsigma(\mathbf{E}_l(t+l|t), \mathbf{u}(t+l-1|t)) \right. \\ &\quad \left. + \varsigma(\mathbf{E}_m, \mathbf{u}(t+m-1|t)) \right\} \\ &\leq -\varsigma(\mathbf{x}(t+1|t), \mathbf{u}(t|t)) + \mathbf{J}_{\text{opt}}^0(t) \\ &\quad + \min \varsigma(\mathbf{E}_m, \mathbf{u}(t+m-1|t)). \end{aligned} \quad (33)$$

In a real distribution system, the system's state  $\mathbf{V}(t+m|t)$  will be in dynamic balance with the desired target state  $\mathbf{V}_{\text{ref}}(t+m|t)$  within certain safety limits in the real distribution system. In order to maintain the stability of the distribution system, the safety limits should be set very small. That means

$E_m$  is close to 0. At the same time, during the MPC optimization process, we select the appropriate coefficient  $\mathbf{F}$  in (28) according to the result of the program running. Through the above analysis and processing, we can approximately constrain the terminal error  $E_m$  to be 0. At this moment, the IACs are not required to provide the active and reactive power needed for the voltage regulation to the distribution system. Therefore, the control input  $\mathbf{u}(t + m - 1|t)$  is 0. Through the above analysis, we can obtain the result as follows:

$$\min \varsigma(\mathbf{E}_m, \mathbf{u}(t + m - 1|t)) = 0. \quad (34)$$

From (31), we can obtain the relationship as follows:

$$\varsigma(\mathbf{E}_1(t + 1|t), \mathbf{u}(t|t)) \geq 0. \quad (35)$$

Combining (34) and (35), (33) can be rewritten as follows:

$$\mathbf{J}_{\text{opt}}^0(t + 1) \leq \mathbf{J}_{\text{opt}}^0(t). \quad (36)$$

Therefore  $\mathbf{J}_{\text{opt}}^0(t)$  is a Lyapunov function of the original system, and the Lyapunov stability of the system at the  $\mathbf{x} = 0$  can be proved. The convergence of MPC is proved.

## REFERENCES

- [1] H. Li, H. Hui, and H. Zhang, "Decentralized energy management of microgrid based on blockchain-empowered consensus algorithm with collusion prevention," *IEEE Trans. Sustain. Energy*, vol. 14, no. 4, pp. 2260–2273, Oct. 2023.
- [2] Y. Wu, V. K. N. Lau, D. H. K. Tsang, L. P. Qian, and L. Meng, "Optimal energy scheduling for residential smart grid with centralized renewable energy source," *IEEE Syst. J.*, vol. 8, no. 2, pp. 562–576, Jun. 2014.
- [3] Z. Zhang, C. Dou, D. Yue, Y. Zhang, B. Zhang, and Z. Zhang, "Event-triggered hybrid voltage regulation with required bess sizing in high-PV-penetration networks," *IEEE Trans. Smart Grid*, vol. 13, no. 4, pp. 2614–2626, Jul. 2022.
- [4] A. S. Yadav and V. Mukherjee, "Conventional and advanced PV array configurations to extract maximum power under partial shading conditions: A review," *Renewable Energy*, vol. 178, pp. 977–1005, 2021.
- [5] A. T. Hoang et al., "Integrating renewable sources into energy system for smart city as a sagacious strategy towards clean and sustainable process," *J. Cleaner Prod.*, vol. 305, 2021, Art. no. 127161.
- [6] M. J. E. Alam, K. M. Muttaqi, and D. Sutanto, "A multi-mode control strategy for VAr support by solar PV inverters in distribution networks," *IEEE Trans. Power Syst.*, vol. 30, no. 3, pp. 1316–1326, May 2015.
- [7] S. Bruno, G. Giannoccaro, C. Iurlaro, M. L. Scala, and M. Menga, "Predictive optimal dispatch for islanded distribution grids considering operating reserve constraints," in *Proc. IEEE 21st Mediterranean Electrotechnical Conf.*, 2022, pp. 518–523.
- [8] J. Hong, H. Hui, H. Zhang, N. Dai, and Y. Song, "Distributed control of large-scale inverter air conditioners for providing operating reserve based on consensus with nonlinear protocol," *IEEE Internet Things J.*, vol. 9, no. 17, pp. 15847–15857, Sep. 2022.
- [9] S. Yang, K.-W. Lao, Y. Chen, and H. Hui, "Resilient distributed control against false data injection attacks for demand response," *IEEE Trans. Power Syst.*, vol. 39, no. 2, pp. 2837–2853, Mar. 2023.
- [10] Q. Xie et al., "Use of demand response for voltage regulation in power distribution systems with flexible resources," *IET Gener. Transmiss. Distrib.*, vol. 14, no. 5, pp. 883–892, 2020.
- [11] S. A. Hosseini, M. Fotuhi-Firuzabad, P. Dehghanian, and M. Lehtonen, "Coordinating demand response and wind turbine controls for alleviating the first and second frequency dips in wind-integrated power grids," *IEEE Trans. Ind. Informat.*, vol. 20, no. 2, pp. 2223–2233, Feb. 2024.
- [12] K. Xie, H. Hui, and Y. Ding, "Review of modeling and control strategy of thermostatically controlled loads for virtual energy storage system," *Protection Control Modern Power Syst.*, vol. 4, no. 4, pp. 1–13, 2019.
- [13] S. Yang, K.-W. Lao, H. Hui, Y. Chen, and N. Dai, "Real-time harmonic contribution evaluation considering multiple dynamic customers," *CSEE J. Power Energy Syst.*, early access, Apr. 20, 2023, doi: [10.17775/CSEE-JPES.2022.06570](https://doi.org/10.17775/CSEE-JPES.2022.06570).
- [14] N. Zhao, S. Gorbachev, D. Yue, C. Dou, and X. Xie, "The effect of communication delays on the frequency stability of power systems integrated with inverter air conditioners," *Sustain. Energy, Grids Netw.*, vol. 32, 2022, Art. no. 100920.
- [15] H. Hui, Y. Ding, T. Chen, S. Rahman, and Y. Song, "Dynamic and stability analysis of the power system with the control loop of inverter air conditioners," *IEEE Trans. Ind. Electron.*, vol. 68, no. 3, pp. 2725–2736, Mar. 2021.
- [16] Y. Hua et al., "Collaborative voltage regulation by increasing/decreasing the operating power of aggregated air conditioners considering participation priority," *Electric Power Syst. Res.*, vol. 199, 2021, Art. no. 107420.
- [17] Y. Hua, Q. Xie, H. Hui, Y. Ding, J. Cui, and L. Shao, "Use of inverter-based air conditioners to provide voltage regulation services in unbalanced distribution networks," *IEEE Trans. Power Del.*, vol. 38, no. 3, pp. 1569–1579, Jun. 2023.
- [18] Y. Wang, Y. Tang, Y. Xu, and Y. Xu, "A distributed control scheme of thermostatically controlled loads for the building-microgrid community," *IEEE Trans. Sustain. Energy*, vol. 11, no. 1, pp. 350–360, Jan. 2020.
- [19] H. Zou, Y. Wang, S. Mao, F. Zhang, and X. Chen, "Online energy management in microgrids considering reactive power," *IEEE Internet Things J.*, vol. 6, no. 2, pp. 2895–2906, Apr. 2019.
- [20] D. Cao, W. Hu, J. Zhao, Q. Huang, Z. Chen, and F. Blaabjerg, "A multi-agent deep reinforcement learning based voltage regulation using coordinated pv inverters," *IEEE Trans. Power Syst.*, vol. 35, no. 5, pp. 4120–4123, Sep. 2020.
- [21] W. Viriyautsahakul, W. Panacharoenwong, W. Pongpiriyakijkul, S. Kosolsaksakul, and W. Nakawiro, "A simulation study of inverter air conditioner controlled to supply reactive power," *Procedia Comput. Sci.*, vol. 86, pp. 305–308, 2016.
- [22] A. Potter, R. Haider, G. Ferro, M. Robba, and A. M. Annaswamy, "A reactive power market for the future grid," *Adv. Appl. Energy*, vol. 9, 2023, Art. no. 100114.
- [23] T. Liu, X. Tan, B. Sun, Y. Wu, and D. H. Tsang, "Energy management of cooperative microgrids: A distributed optimization approach," *Int. J. Electr. Power Energy Syst.*, vol. 96, pp. 335–346, 2018.
- [24] D. Blum et al., "Field demonstration and implementation analysis of model predictive control in an office HVAC system," *Appl. Energy*, vol. 318, 2022, Art. no. 119104.
- [25] Z. Li et al., "A tube model predictive control based cyber attack-resilient optimal voltage control strategy in wind farms," *CSEE J. Power Energy Syst.*, vol. 10, no. 2, pp. 530–538, Mar. 2024.
- [26] N. Zhao et al., "Model predictive based frequency control of power system incorporating air-conditioning loads with communication delay," *Int. J. Electr. Power Energy Syst.*, vol. 138, 2022, Art. no. 107856.
- [27] C.-H. Lin, W.-L. Hsieh, C.-S. Chen, C.-T. Hsu, T.-T. Ku, and C.-T. Tsai, "Financial analysis of a large-scale photovoltaic system and its impact on distribution feeders," *IEEE Trans. Ind. Appl.*, vol. 47, no. 4, pp. 1884–1891, Jul./Aug. 2011.
- [28] H. Hui, Y. Ding, and M. Zheng, "Equivalent modeling of inverter air conditioners for providing frequency regulation service," *IEEE Trans. Ind. Electron.*, vol. 66, no. 2, pp. 1413–1423, Feb. 2019.
- [29] H. Hui et al., "A transactive energy framework for inverter-based HVAC loads in a real-time local electricity market considering distributed energy resources," *IEEE Trans. Ind. Informat.*, vol. 18, no. 12, pp. 8409–8421, Dec. 2022.
- [30] D. Wang, K. Meng, X. Gao, J. Qiu, L. L. Lai, and Z. Y. Dong, "Coordinated dispatch of virtual energy storage systems in LV grids for voltage regulation," *IEEE Trans. Ind. Informat.*, vol. 14, no. 6, pp. 2452–2462, Jun. 2018.
- [31] A. T. Eseye, B. Knueven, X. Zhang, M. Reynolds, and W. Jones, "Resilient operation of power distribution systems using MPC-based critical service restoration," in *Proc. IEEE Green Technol. Conf.*, 2021, pp. 292–297.
- [32] S. Gorbachev et al., "MPC-based LFC for interconnected power systems with PVA and ESS under model uncertainty and communication delay," *Protection Control Modern Power Syst.*, vol. 8, no. 4, pp. 1–17, Oct. 2023.
- [33] Z. Chen, Z. Du, and H. Zhan, "An optimal volt/var control strategy for an islanded microgrid considering the volt/var control capability," in *Proc. 8th Renewable Power Gener. Conf.*, 2019, pp. 1–6.
- [34] Z. Zhang, D. Yue, and C.-X. Dou, "DMPC-based coordinated voltage control for integrated hybrid energy system," *IEEE Trans. Ind. Informat.*, vol. 17, no. 10, pp. 6786–6797, Oct. 2021.
- [35] M. Thornton, M. Motalleb, H. Smidt, J. Branigan, and P. Siano, "Internet-of-things hardware-in-the-loop simulation architecture for providing frequency regulation with demand response," *IEEE Trans. Ind. Informat.*, vol. 14, no. 11, pp. 5020–5028, Nov. 2018.
- [36] V. B. Vales, O. C. Fernández, T. Domínguez-Bolaño, C. J. Escudero, and J. A. García-Naya, "Fine time measurement for the Internet of Things: A practical approach using ESP32," *IEEE Internet Things J.*, vol. 9, no. 19, pp. 18305–18318, Oct. 2022.